An *in situ* structural study of the high-pressure transformations in $TiH_{0.74}$

2002 J. Phys.: Condens. Matter 14 955

(http://iopscience.iop.org/0953-8984/14/5/301)

INSTITUTE OF PHYSICS PUBLISHING JOURNAL OF PHYSICS: CONDENSED MATTER

J. Phys.: Condens. Matter **14** (2002) 955–966 PII: S0953-8984(02)28225-9

An *in situ* structural study of the high-pressure transformations in $TiH_{0.74}$

I O Bashkin[1], V K Fedotov[1], H-J Hesse[2], A Schiwek[2], W B Holzapfel[2] and E G Ponyatovsky[1]

[1] Institute of Solid State Physics, Russian Academy of Sciences, Chernogolovka, Moscow Province, 142432, Russia
[2] Fachbereich 6–Physik, Universität–GH Paderborn, D–33095 Paderborn, Germany

Received 2 February 2001
Published 25 January 2002
Online at stacks.iop.org/JPhysCM/14/955

E-mail: bashkin@issp.ac.ru

Abstract

Structural phase transitions in the $TiH_{0.74}$ alloy have been studied in the pressure range extending to 30.5 GPa at temperatures of up to 630 K, using diamond anvils and energy dispersive x-ray diffraction. Two phase transitions were observed at high pressures. At room temperature, the $TiH_{0.74}$ alloy undergoes a transition to the (η+ω) two-phase state at above 7 GPa, and then this state persists up to 30.5 GPa. The other phase transition occurs upon heating (η+ω)-$TiH_{0.74}$ to $T > 560$ K to give a single-phase state, ζ-$TiH_{0.74}$. The ω-phase corresponds to the high-pressure phase of pure titanium. The Ti sublattices of the η- and ζ-phases are indexed within the tetragonal symmetry, their specific volumes being much the same. Analysis of the specific volumes and the hydrogen contents in these two phases suggests that hydrogen atoms are likely to occupy tetrahedral interstices in the ζ-phase and octahedral interstices in the η-phase.

1. Introduction

The main feature of the T–c phase diagram of the Ti–H system at atmospheric pressure (figure 1) is the β–(α+δ) eutectoid transformation at 573 K, in which the high-temperature phase—a solid solution of hydrogen in the body-centred cubic (BCC) β-Ti sublattice—is in equilibrium with a solid solution of hydrogen in the hexagonal close-packed (HCP) α-Ti sublattice, and the non-stoichiometric dihydride δ-TiH_{2-y}, with a face-centred cubic (FCC) metal sublattice [1, 2]. Closer to the stoichiometric composition, the FCC dihydride undergoes a transition to the ε-TiH_{2-y} phase with a face-centred tetragonal (FCT) metal sublattice and axial ratio $c/a < 1$. Hydrogen atoms in all these phases are randomly distributed over tetrahedral interstitial sites (tetrasites) [1–3]. There is one more phase, monohydride γ-TiH, found to be stable under atmospheric pressure [4–6]. A neutron diffraction study of γ-TiD [3, 7] demonstrated that Ti atoms form a face-centred orthorhombic sublattice with axial ratios

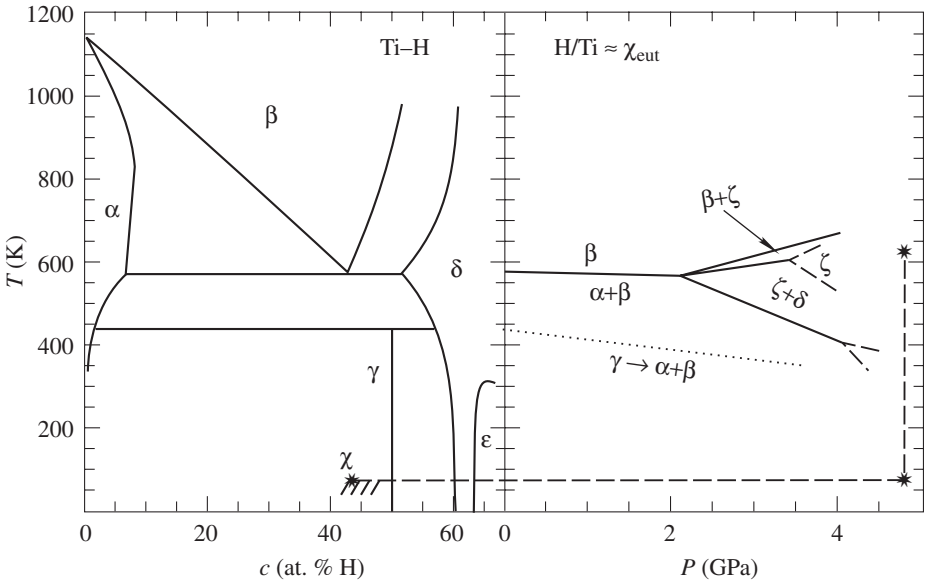

Figure 1. Phase diagram of the Ti–H system [2]. The left-hand part shows the T–c projection at atmospheric pressure, and the right-hand part is the T–P projection for nearly eutectoid hydrides. The high-pressure quenching of the ζ-phase is represented by the broken curve, and the metastability region of the resulting χ-phase is hatched. The low-temperature boundary of the ζ-phase stability region (right-hand part) ends with a broken fork in order to indicate that one more phase transition is likely to occur under these conditions. The $\gamma \rightarrow (\alpha{+}\delta)$ transition line on heating [8] is shown by a dotted curve.

$b/a \approx 1.015$ and $c/a \approx 1.09$, with hydrogen atoms occupying tetrasites on alternate (110) planes. Heating to 440 K irreversibly transforms the γ-phase into the $(\alpha{+}\delta)$ two-phase state [4, 5].

Under pressure, the eutectoid temperature and the transition temperature of the γ-phase decrease, as shown in the right-hand part of figure 1, and a new phase, ζ, appears in the alloys near the eutectoid point at $P = 2.05$ GPa, $x = \mathrm{H/Ti} \approx 0.74$ and $T \approx 560$ K [2, 6, 8]. Early structural studies of the ζ-phase were limited to x-ray measurements [8], and several diffraction patterns were registered photographically between $P = 5$–8 GPa and $T = 520$–620 K. It was reported that Ti atoms in the ζ-phase form an FCT sublattice with axial ratio $c/a = 0.89$ [8]. Further studies attempted to obtain the high-pressure phase by thermobaric treatment, which involved thermal treatment of the TiH_x samples at $T \geqslant 560$ K and $P \geqslant 5$ GPa, quenching to liquid nitrogen temperature, and recovery to atmospheric pressure (see figure 1). The quenched samples were single-phase, and this state, designated as the χ-phase, was metastable under atmospheric pressure below 95 K [6]. Extensive studies of the quenched metastable state at $T \leqslant 90$ K by the neutron scattering technique [2, 3, 7, 9] have shown that hydrogen atoms in the χ-phase randomly occupy octahedral interstitial sites (octasites) of the FCT Ti sublattice, whereas the tetrasites are occupied in the stable phases. Since the specific volumes of the ζ- and χ-phases are very similar and both are by about 10% less than the volumes of the other hydride phases in the Ti–H system, it was assumed that the ζ-phase also has hydrogen distributed over octasites [8, 9]. However, several experimental facts have been reported, which distinguish the ζ-phase from the χ-phase. First, the axial ratio in the χ-phase, $c/a = 0.95$ [9], is much closer to unity than that in the ζ-phase, $c/a = 0.89$ [8]. Second, TiH_x and TiD_x alloys are

superconducting under high pressure, as well as after a thermobaric treatment, but the pressure dependence of the superconducting transition temperature of the TiD_x samples, measured *in situ*, [10] shows significantly lower T_c values than in the case of the thermobaric treatment [11].

To elucidate the high-pressure phase diagram of the TiH_x alloys near the eutectoid composition, direct *in situ* x-ray diffraction measurements under high pressure were performed in the present study.

2. Experimental details

The initial two-phase alloy of the eutectoid composition was prepared by direct reaction of Ti metal (total impurities < 0.02 at. %) with hydrogen gas obtained by thermal decomposition of TiH_2 (for details see [12]). The hydrogen content was determined from the weight gain, $H/Ti = 0.74 \pm 0.01$. To obtain smaller grains, the alloy was brought to the χ-state using the treatment described above and low-temperature quenching under pressure, and then heated rapidly to ambient conditions. After this treatment, the characteristic grain size of Ti precipitates in the γ-TiH matrix was less than 100 Å [13]. After being ground immediately before measurements, $TiH_{0.74}$ samples were transformed into the (α+δ) two-phase state by heating to 600 K. Energy dispersive x-ray diffraction (EDXD) was performed with synchrotron radiation at HASYLAB (DESY, Hamburg). A diamond anvil high-pressure cell with flats 500 μm in diameter was used. $TiH_{0.74}$ samples were finely ground and placed together with several ruby chips in a hole 150 μm in diameter in the Inconel gasket, filled with white mineral oil as a pressure transmitting medium [14, 15]. The pressure was measured by the ruby luminescence technique [16]. Temperature was varied by means of an external electric heater. The temperature stability during each exposure was ± 3 K. The diffraction spectra were collected with a Ge detector at a scattering angle of $2\Theta \approx 9.48^\circ$.

3. Results

Two *in situ* experiments were necessary to find the general features characterizing the $T-P$ behaviour of the $TiH_{0.74}$ alloy. The first experiment was a compression/decompression run carried out with $TiH_{0.74}$ at room temperature. The evolution of the EDXD spectra upon compression is illustrated in figure 2. For convenience of comparison, only the low-energy parts of the spectra are shown. A normal behaviour of the two-phase (α+δ)-$TiH_{0.74}$ sample is observed between 0 and 6.0 GPa. The reflection appearing in the 7.6 GPa spectrum at 32 keV points to the onset of a phase transition. This is in close agreement with a pressure of 7.5 GPa obtained by extrapolation of previous data on the (α+δ) $\rightarrow \zeta$ transformation [6, 8] to room temperature. The curve corresponding to this transformation was plotted in [6, 8] using differential thermal analysis at elevated temperatures, but it was not extended to 300 K because of the decelerated transformation kinetics. The next spectrum taken at 9.4 GPa shows no indications of the previously existing α- and δ-phases, but the diffuse peak at around 35.4 keV and the very high relative intensity of the peak at around 31.5 keV indicate an intermediate state of the alloy. The formation of the high-pressure state is complete at 12.8 GPa, and all spectral features exhibit normal behaviour at higher pressures up to the experimental limit of 30.5 GPa.

The $TiH_{0.74}$ behaviour is reversible upon decompression. The low-pressure diffraction pattern is restored when the pressure is lowered from 4.1 to 1.6 GPa, in qualitative agreement with earlier resistivity measurements [6, 8] in which a resistivity jump due to a reverse

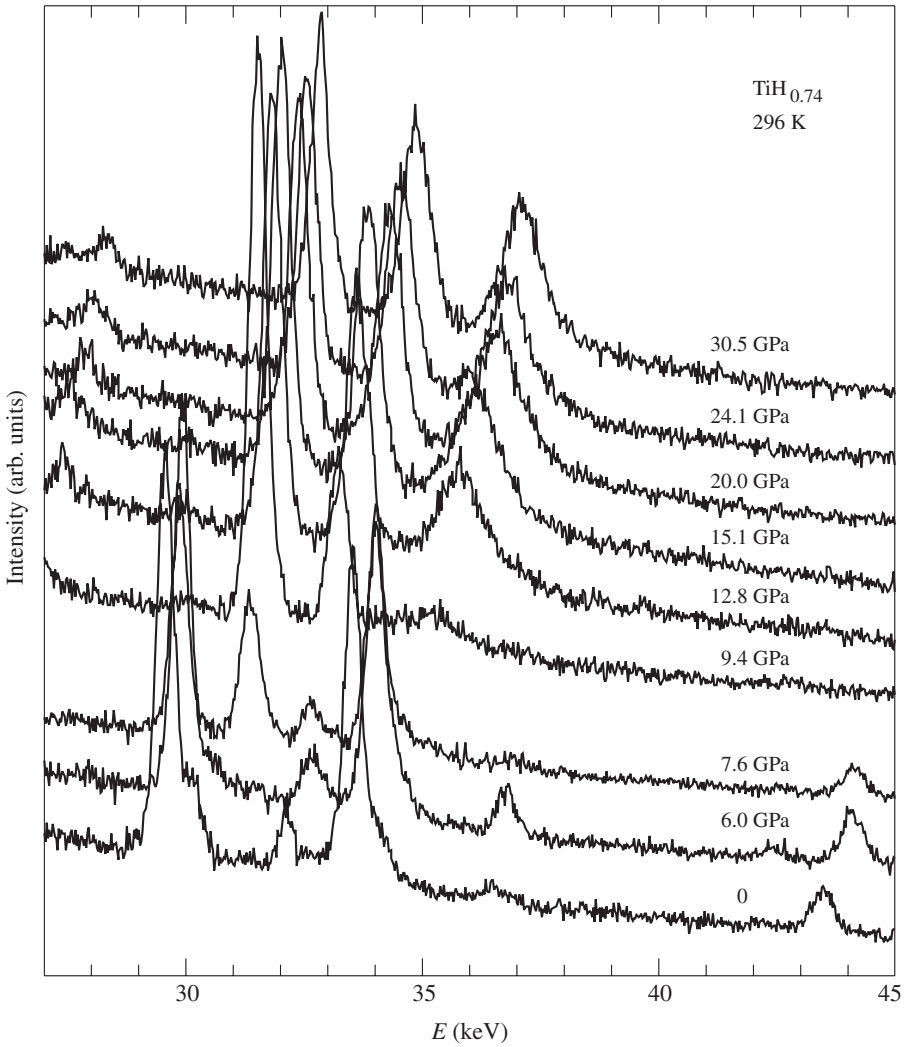

Figure 2. EDXD spectra of $TiH_{0.74}$ at room temperature and different pressures. Only the range of intense reflections at low energies is shown.

transformation has been observed between 5.2 and 4.6 GPa.

The diffraction pattern of the high-pressure state observed at room temperature consisted of three strong peaks below 38 keV and several low-intensity peaks at higher energies. The positions of the strong peaks could not be described in terms of a single unit cell with reasonable lattice parameters. This was indicative of a two-phase state of the $TiH_{0.74}$ alloy under high pressure at 300 K. The second experiment including the heating/cooling runs at starting pressures of 6.3 and 11.5 GPa, i.e. in the previously reported range corresponding to the ζ-phase, helped to elucidate the structure of the high-pressure state.

The evolution of the diffraction spectra during these heating/cooling cycles is presented in figures 3 and 4. Both figures demonstrate a considerable change in the pattern above about 550 K. In order to interpret the changes observed in these runs, multiphase diffraction spectra were simulated and fitted to the experimental intensities with an accuracy of about 15% using

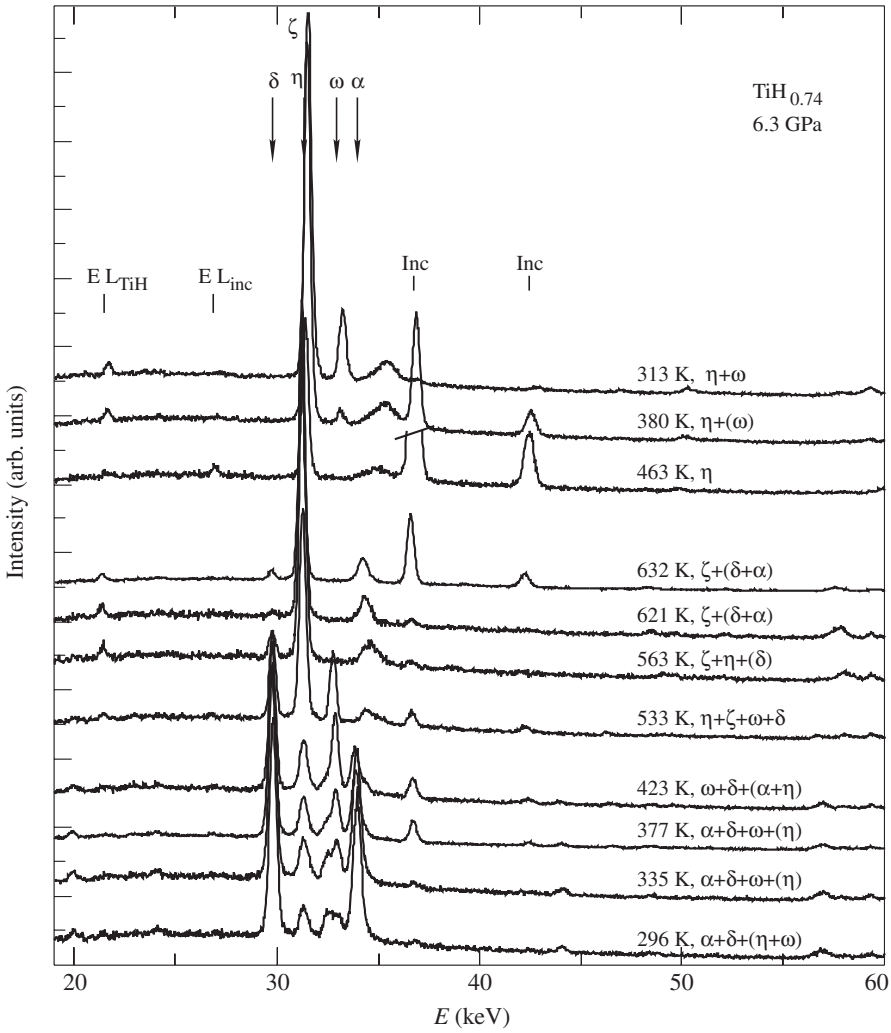

Figure 3. Evolution of the EDXD spectra of $TiH_{0.74}$ upon heating to 632 K and cooling at a nominal pressure of 6.3 GPa (bottom to top). The indicated phase contents are obtained as described in the text. Marked are positions of the escape lines, the Inconel reflections and the most intense reflections of the TiH_x phases.

the DBWS-9411 computer program. A better fit was impossible owing to the rather small number of sample grains and the resulting insufficient statistics of grain orientations. The simulation was based on the initial low-pressure α- and δ-phases, two high-pressure phases, ζ-$TiH_{0.74}$ and ω-Ti [17], Inconel and a new FCT high-pressure phase, η. The last phase was necessary in order to describe the spectral features below about 570 K.

The diffraction pattern becomes simplest upon heating to 618 K at 11.5 GPa. The experimental EDXD spectrum obtained under these conditions (the upper full curve in figure 5) can be described as a superposition of the diffraction pattern of the FCT ζ-phase (the bottom full curve) and two Inconel reflections. The lattice parameters of the FCT unit cell, $a = 4.253$ Å and $c = 3.854$ Å ($c/a = 0.906$), from the present fit are comparable with earlier data, $a = 4.334$ Å, $c = 3.851$ Å and $c/a = 0.89$ [8].

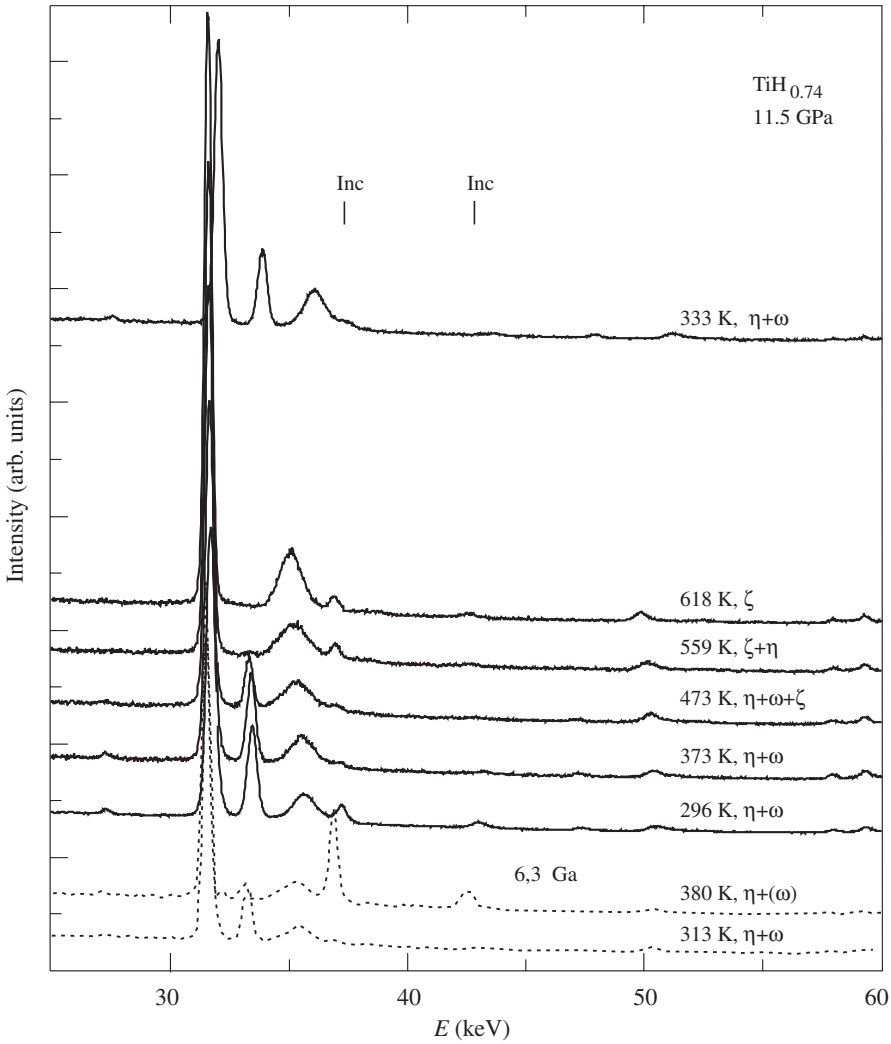

Figure 4. EDXD spectra of $TiH_{0.74}$ upon heating to 618 K and cooling at a nominal pressure of 11.5 GPa (full curves). The indicated phase contents are obtained as described in the text. For comparison, the EDXD spectra taken on cooling at 6.3 GPa are presented as dotted curves at the bottom.

The main difference between the high- and room-temperature EDXD spectra at 11.5 GPa is a prominent peak around 33.5 keV that appears in the latter spectrum in the position of the (101)+(110) reflection of the ω-phase (see also figure 6). The existence of the ω-phase at room temperature is supported by a minor peak at 27.3 keV, corresponding to the $(001)_\omega$ reflection. Other ω-phase peak positions (see the broken curve in figure 6) also correlate with the features in the experimental spectrum. With the contribution from the ω-phase at room temperature taken into account, one can notice that the strongest reflection in figure 5, corresponding to the (111) line of the ζ-phase at 618 K, remains nearly in the same position at $T = 296$ K, whereas other reflections of lower intensity are shifted somewhat. Therefore, the room-temperature EDXD spectrum can be described most reasonably as a superposition of the diffraction patterns

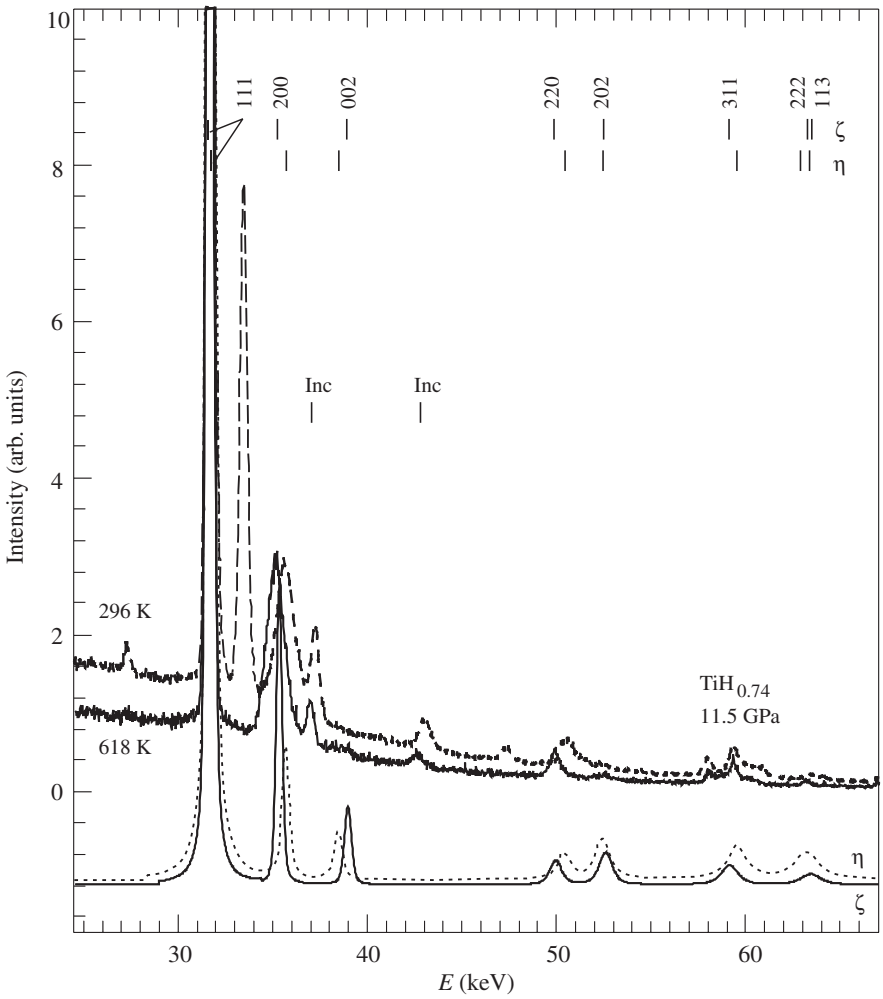

Figure 5. EDXD spectra of $TiH_{0.74}$ at $T = 618$ K and $T = 296$ K in a heating run at $P = 11.5$ GPa (top curves) and simulated diffraction patterns of the ζ- and η-phases (bottom curves). Full curves represent the data obtained at $T = 618$ K, broken curves are for $T = 296$ K. Indexes are given for the FCT unit cell of the ζ-phase.

of the ω-phase ($a = 4.490$ Å, $c = 2.753$ Å and $c/a = 0.613$), a new FCT phase, η, with the unit cell parameters $a = 4.214$ Å and $c = 3.909$ Å ($c/a = 0.928$) and two Inconel reflections. The simulated diffraction pattern of the η-phase is represented by the broken curve in figure 5 and by the full curve in figure 6. The spectral changes occurring upon heating from room temperature to 618 K (figure 4) can be discussed in terms of the two-phase (η+ω)-state of the $TiH_{0.74}$ alloy below 373 K, the (η+ω) $\rightarrow$ ζ phase transformation at about 470 to 560 K and the single-phase state, ζ, above this transformation. This phase transition is reversible upon cooling, but a shift of all the reflections to higher energies indicates some lattice contraction. This contraction is well accounted for by an increase in pressure to 17.4 GPa after cooling, as a result of a mechanical relaxation of the diamond cell upon cooling.

Two broken curves presented at the bottom of figure 4 are the EDXD spectra measured on cooling in the first heating/cooling cycle. Their similarity to the EDXD spectra obtained

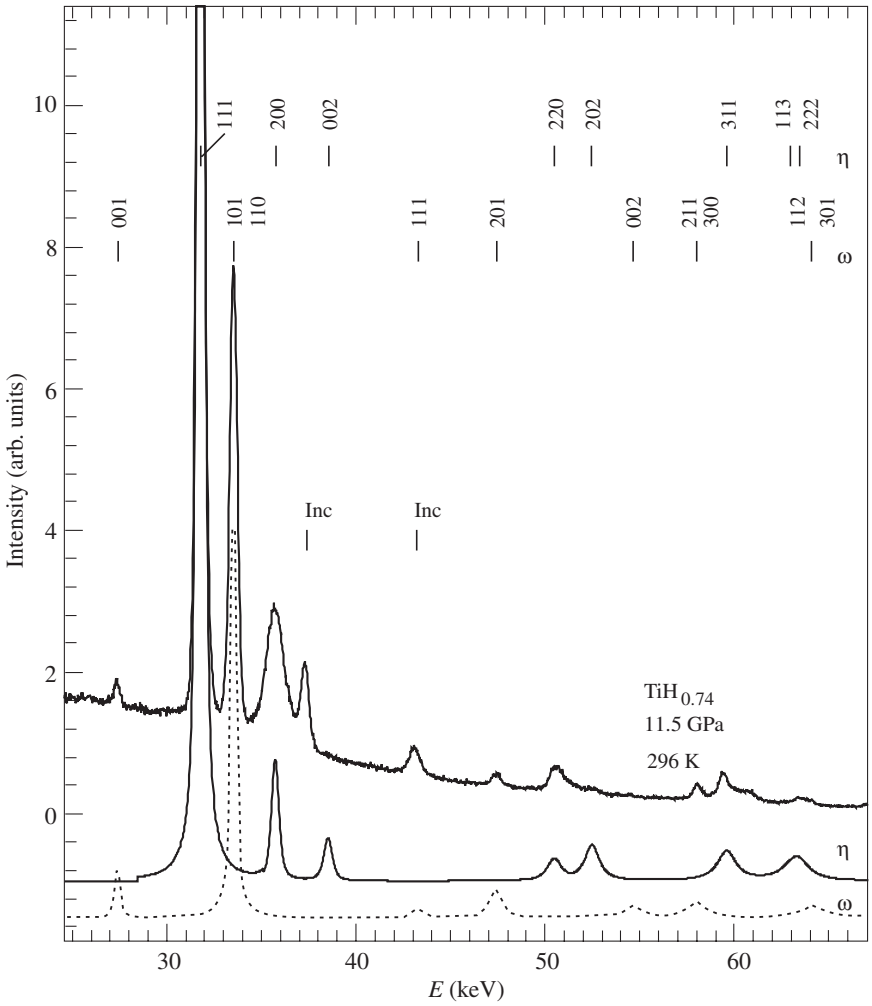

Figure 6. EDXD spectrum of $TiH_{0.74}$ at $T = 296$ K and $P = 11.5$ GPa (top curve) and simulated diffraction patterns of the η-phase (full curve at the bottom) and the ω-phase (broken curve).

below 380 K in the second cycle is obvious. This indicates already qualitatively that the sample transforms to the (η+ω) two-phase state by the end of the first cycle. Figure 7 shows that at the beginning of the first run ($T = 300$ K and $P = 6.3$ GPa) the $TiH_{0.74}$ alloy consists of four phases, i.e., the initial α- and δ-phases is partially transformed to the ω- and η-phases. The amount of the initial phases decreases upon heating, but their trace amounts are present even at $T = 632$ K. Any traces of the initial phases disappear completely upon cooling, and the main reflections are shifted somewhat to higher energies. This is again a consequence of a spontaneous pressure increase (to 9.2 GPa) due to mechanical relaxation. The irreversibility of the (α+δ) $\rightarrow$ (η+ω) $\rightarrow$ ζ transitions at 6.3 GPa was also expected because of the hysteresis of the (α+δ)–(η+ω) transition.

The present data elucidate quite a number of phenomena observed previously in the Ti–H system. It has been reported on studying the T–P diagrams of the near-eutectoid TiH_x hydrides [6, 8] that the resistivity and the thermal anomalies concomitant with the (α+δ) $\rightarrow$ ζ

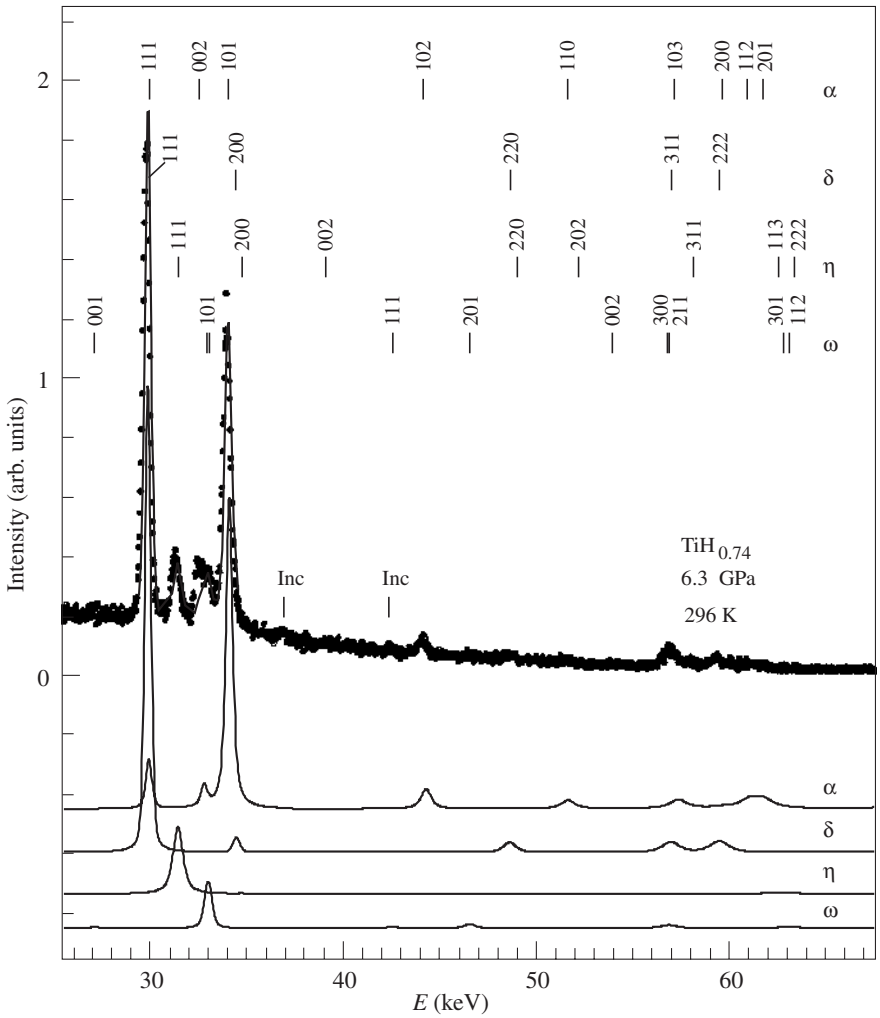

Figure 7. EDXD spectrum of $TiH_{0.74}$ at $T = 296$ K and $P = 6.3$ GPa (points) and simulated contributions from the α-, δ-, η- and ω-phases (full curves at the bottom). The full curve drawn through the experimental points is a sum of the calculated contributions.

transformation *split* when the transformation temperature decreases to 450–500 K in the pressure range of 4.1–4.8 GPa. The occurrence of another high-pressure phase in addition to ζ was therefore assumed (see also figure 1). The present data unambiguously show that the second high-pressure phase, η, does occur in the Ti–H system and transforms to the ζ-phase upon heating. The near-eutectoid $TiH_{0.74}$ alloy is in the (η+ω) two-phase state over a range from about 7.6 GPa up to 30.5 GPa at room temperature, whereas the high-temperature state is single-phase. The occurrence of the ω-phase indicates that the chemical composition of the η-phase is $x > 0.74$. Further conclusions about the η-phase composition can be made on considering the specific volumes.

The volumes per formula unit of ζ-$TiH_{0.74}$ and η-TiH_x, calculated from the FCT lattice parameters at 11.5 GPa, are nearly the same, $V_\zeta = 17.43$ Å^3 and $V_\eta = 17.35$ Å^3. This similarity is consistent with the fact that the slope of the ζ–(η+ω) equilibrium line in the T–P

plane is not too steep. However, this circumstance disagrees with the normal behaviour of metals upon hydrogenation. A normal $V(x)$ dependence observed for many d-metal hydrides is a linear expansion of the metal sublattice with a slope of $\partial V/\partial x = 1.5$–$3$ Å^3 [18, 19]. This empirical rule is not observed in the case of the ζ- and η-phases, although they have the same symmetry of the metal sublattice. It can be assumed that this violation is due to different hydrogen occupancies in the ζ- and η-phases, i.e. a changeover of the hydrogen occupancy type to octahedral occurs only in the low-temperature η-phase, whereas the ζ-phase has hydrogen distributed over tetrasites, as in phases stable under atmospheric pressure. Since the number of octasites per unit cell in the FCT lattice is unity, the hydrogen content in the η-phase must not exceed $x = 1$.

Now the Ti–H system appears to be a metal–hydrogen system with a rather simple phase diagram at atmospheric pressure and unique phase transformations under high pressure, related to a change of the hydrogen occupancy type. The tetra–octa hydrogen transition in the Ti–H system under high pressure is related to the crystal-chemical criterion [20] which states that tetrasites are preferable positions for hydrogen occupation when the metal radius is larger than about 1.4 Å, and octasites become preferable at smaller metal radii. The Ti metal radius is somewhat larger than the critical value, and, therefore, hydrogen occupies tetrasites in titanium hydrides at atmospheric pressure, but octasites become advantageous upon compression to above 7.5 GPa at 300 K. The occurrence of the high-pressure tetra–octa hydrogen transition indicates that the energy difference between the hydrogen states in tetra- and octasites is not large. This is why the entropy factor in the Gibbs energy can also affect the preference of the interstitial type and may result in an octa–tetra hydrogen transition upon heating under pressure.

The occurrence of the ζ–(η+ω) phase transformation upon heating under pressure provides an insight into the nature of the χ-phase and accounts for the superconductivity data [10, 11] reproduced in figure 8. The T_c value for the metastable χ-$TiD_{0.74}$ is 5 K at atmospheric pressure [11], whereas extrapolation of a linear $T_c(P)$ dependence for $TiD_{0.74}$ from $P > 10$ GPa to atmospheric pressure gives $T_c = 4$ K [10]. It is clear now that the *in situ* data [10] with compression at 290 K are related to (η+ω)-$TiD_{0.74}$. The superconductivity of $TiD_{0.74}$ under these conditions is associated with the η-phase with $x > 0.74$. A strongly different phase composition of the $TiD_{0.74}$ alloy is obtained after low-temperature quenching from the ζ-phase region. No long-range hydrogen diffusion occurs upon such quenching, owing to the low hydrogen mobility, and, therefore, phase separation resulting in precipitation of the ω-phase is not the case. However, displacement of hydrogen atoms from the tetrasites to the octasites within the same unit cell is facilitated, compared with the case of long-range diffusion. This kind of hydrogen displacement upon high-pressure quenching of the ζ-phase seems to be a mechanism by which the χ-phase with hydrogen atoms randomly distributed over octasites and a chemical composition coinciding with the average hydrogen content in the alloy ($x = 0.74$ in the given case) is formed. Thus, the T_c values for the χ-phase and the η-phase may be different.

Finally, the present indexing of the high-pressure diffraction patterns may need some discussion. Preparation of a small isotropic sample for these measurements presents a serious experimental problem. The insufficient statistics of grain orientations in the samples results in that the relative intensities of the x-ray reflections cannot be accurately fitted even for the initial (α+δ) composition. The accuracy of fitting is illustrated in figure 7 where the intensity of the (002) reflection of the α-phase is distinctly underestimated. Similarly, the tetragonal metal sublattices chosen for the ζ- and η-phases are the lattices of highest symmetry, adequately describing the peak positions. Diffraction measurements with better statistics of grain orientations may lead to further refinement of the crystal structure of these phases.

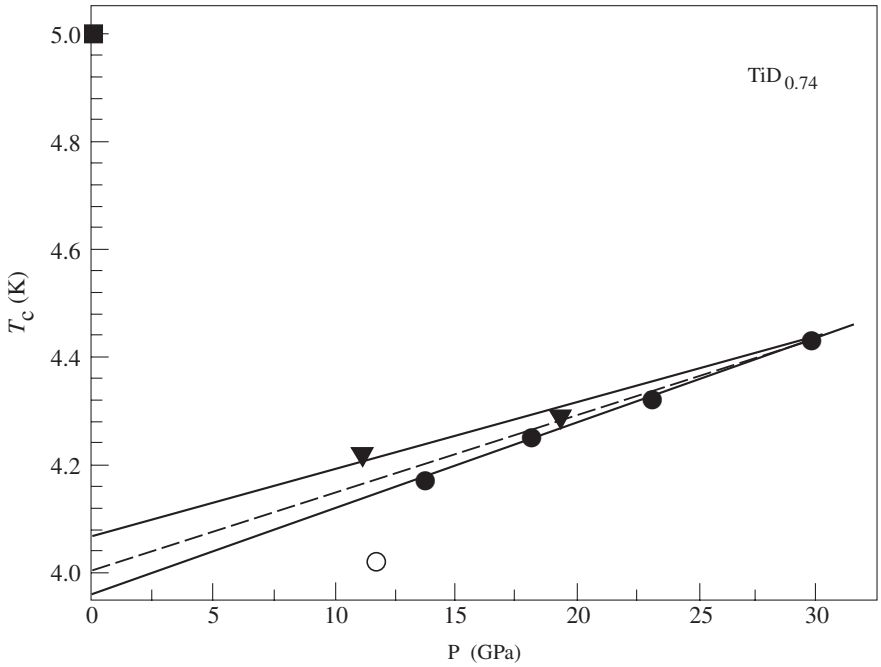

Figure 8. Effect of pressure on the superconducting transition temperature of $TiD_{0.74}$, found from magnetic susceptibility measurements [10, 11]. The superconducting transitions for compression and decompression [10] are shown by circles and triangles, respectively. The first compression point is open because it breaks the general trend. The T_c value of quenched χ-$TiD_{0.74}$ [11] is shown by a square.

4. Conclusions

The present *in situ* study of the crystal structure of $TiH_{0.74}$ demonstrated that the near-eutectoid alloys in the Ti–H system undergo a phase transition to the (η+ω) two-phase state at pressures exceeding 7 GPa at room temperature, which remains stable up to at least 30.5 GPa. Another phase transition resulting in a single-phase state, the ζ-phase, is observed upon heating to $T = 470$ to 560 K. Both high-pressure phases have tetragonal or nearly tetragonal sublattices of metal atoms and nearly the same specific volumes, the hydrogen content of the η-phase being higher than that in the ζ-phase. The relationships between the specific volumes and the chemical compositions are accounted for by different hydrogen occupancies, i.e. the hydrogen atoms seem to occupy tetrahedral interstices in the ζ-phase and octahedral interstices in the η-phase. The assumption of the octahedral occupancy for hydrogen in the η-phase is in agreement with the enhanced superconductivity of the η-phase, as is the case for the χ-phase where the hydrogen distribution over the octasites has been confirmed by neutron scattering studies.

Acknowledgments

This work was supported by the Russian Foundation for Basic Research Grant No 00-02-17562. HASYLAB experiments were performed under Project No II-96-76.

References

[1] San–Martin A and Manchester F D 1987 *Bull. Alloy Phase Diagrams* **8** 30
[2] Bashkin I O, Kolesnikov A I and Ponyatovsky E G 1995 *High Press. Res.* **14** 91
[3] Kolesnikov A I, Balagurov A M, Bashkin I O, Fedotov V K, Malyshev V Yu, Mironova G M and Ponyatovsky E G 1993 *J. Phys.: Condens. Matter.* **5** 5045
[4] Bashkin I O, Gurov A F, Malyshev V Yu and Ponyatovsky E G 1992 *Sov. Phys. Solid State* **34** 1386
[5] Bashkin I O, Malyshev V Yu and Ponyatovsky E G 1993 *Z. Phys. Chem.* **179** 111
[6] Bashkin I O, Malyshev V Yu and Ponyatovsky E G 1993 *Z. Phys. Chem.* **179** 289
[7] Balagurov A M, Bashkin I O, Kolesnikov A I, Malyshev V Yu, Mironova G M, Ponyatovsky E G and Fedotov V K 1991 *Sov. Phys. Solid State* **33** 711
[8] Bashkin I O, Dyuzheva T I, Lityagina L M and Malyshev V Yu 1993 *Phys. Solid State* **35** 1528
[9] Bashkin I O, Kolesnikov A I, Ponyatovsky E G, Balagurov A M and Mironova G M 1995 *Phys. Solid State* **37** 2065
[10] Bashkin I O, Nefedova M V, Tissen V G and Ponyatovsky E G 1998 *Phys. Solid State* **40** 1950
[11] Bashkin I O, Malyshev V Yu, Rashchupkin V I and Ponyatovsky E G 1988 *Sov. Phys. Solid State* **30** 1155
[12] Bashkin I O, Gurov A F, Malyshev V Yu and Ponyatovsky E G 1992 *Sov. Phys. Solid State* **34** 674
[13] Bashkin I O, Kolesnikov A I, Malyshev V Yu, Ponyatovsky E G, Borbély S, Rosta L and Pépy G 1993 *J. de Physique IV* (Colloque C8, Suppl. J. de Physique I, No. 12) **3** 287
[14] Syassen K and Holzapfel W B 1975 *Europhys. Conf. Abstr. Ser. 1A* p 75
[15] Holzapfel W B 1978 in *High Pressure Chemistry* ed H Kelm (Boston: D Reidel) p 177
[16] Mao H K, Bell P M, Shaner J W and Steinberg D J 1978 *J. Appl. Phys.* **49** 3276
[17] Tonkov E Yu 1992 *High Pressure Phase Transformations* vol. 2 (Philadelphia: Gordon and Breach Science Publishers) p 682
[18] Peisl H 1978 in *Hydrogen in Metals I*, *Topics in Appl. Phys.* vol. 28 ed G Alefeld and J Völkl (Berlin: Springer) p 53
[19] Fukai Y 1993 *The Metal–Hydrogen System* (Berlin: Springer) p 95
[20] Irodova V A, Somenkov V A and Shilshtein S Sh 1983 *Sov. Phys. Solid State* **25** 3196